

**CHAPTER V**  
**PREPARATION AND CHARACTERIZATION OF Cd-Fe-S THIN**  
**FILMS**

<b>5.1 INTRODUCTION</b>	100
<b>5.2 EXPERIMENTAL</b>	100
<i>5.2.1 Thin Film deposition</i>	100
5.2.1.1 Substrate cleaning.	100
5.2.1.2 Preparation of solution	100
5.2.1.3 Deposition of Cd-Fe-S thin films.	101
5.2.1.4 Spray rate	102
5.2.1.5 Substrate temperature	102
5.2.1.6 Concentration of spraying solution	103
<i>5.2.2 Characterization of Cd-Fe-S thin films</i>	103
5.2.2.1 X-ray diffraction	103
5.2.2.2 Energy dispersive X-ray spectroscopy (EDAX)	103
5.2.2.3 Optical microscopy	103
5.2.2.4 Optical absorption	104
5.2.2.5 Electrical resistivity	104
5.2.2.6 Thermoelectric Power (TEP)	104
<b>5.3 RESULTS AND DISCUSSION</b>	104
<i>5.3.1 X-ray diffraction</i>	104
<i>5.3.2 Energy dispersive x-ray spectroscopy (EDAX)</i>	106
<i>5.3.3 Optical microscopy</i>	107
<i>5.3.4 Optical absorption</i>	107
<i>5.3.5 Electrical resistivity</i>	110
<i>5.3.6 Thermoelectric Power (TEP)</i>	114
<b>REFERENCES</b>	116

## 5.1 INTRODUCTION

Recently, considerable attention is being given to the preparation of metal chalcogenide thin films for [1-3]. A number of binary and ternary semiconductors such as CdS, CdSe, Cd Te, Cd Bi<sub>2</sub>S<sub>4</sub>, CdSb<sub>2</sub>S<sub>4</sub>, CdSe<sub>x</sub>S<sub>1-x</sub>, Cd<sub>x</sub>Zn<sub>1-x</sub>S etc. have been prepared by the spray pyrolysis technique [4-11]. However there is no report available on the preparation of Cd-Fe-S material in bulk or thin film form.

The preparation of Cd-Fe-S thin films onto glass substrates and their structural, optical and electrical characterization has been reported and discussed in this chapter.

## 5.2 EXPERIMENTAL

### 5.2.1 THIN FILM DEPOSITION

Cd-Fe-S thin films have been deposited onto commercially available glass substrates using spray pyrolysis technique as discussed in section 3.2.1.1

#### 5.2.1.1 Substrate cleaning

The procedure described in section 3.2.1.2 has been used to clean the substrates.

#### 5.2.1.2 Preparation of solution

Double distilled water has been used to prepare all the solutions. The initial ingredients used were

- 1) G.R. Grade Cadmium chloride ( $\text{CdCl}_2 \cdot \text{H}_2\text{O}$ ) supplied by Loba chemie, Mumbai.
- 2) A.R. Grade thiourea ( $\text{NH}_2\text{-CS-NH}_2$ ) supplied by Loba chemie, Mumbai.
- 3) A.R. Grade ferrous chloride ( $\text{FeCl}_2$ ) supplied by Loba chemie, Mumbai.

All the solutions with 0.1 M concentration were prepared separately by dissolving appropriate amount of chemicals into double distilled water to get the required volume.

#### *5.2.1.3 Deposition of Cd-Fe-S thin films*

Thin films of Cd-Fe-S were deposited by spraying mixture of the solutions of cadmium chloride (0.05 M), thiourea (0.05 M) and ferrous chloride (0.05 M) onto preheated glass substrates maintained at desired temperature. For each deposition, the quantity of solution to be sprayed was maintained fixed to be 20 cc.

The films were deposited for various volumetric proportions of Cd:Fe. Keeping the volume of sulfur precursor (thiourea) solution constant (10 cc), the volumetric proportion of Cd and Fe was varied. By studying various properties of the films, the effect of Fe content in Cd-Fe-S is tested.

After deposition, the films were allowed to cool to a room temperature and then taken out of the spray pyrolysis chamber.

#### 5.2.1.4 *Spray rate*

The Spray rate is one of the most important preparative parameters in thin film deposition by the spray pyrolysis technique. The spray rate can be varied either by changing the air pressure (carrier gas ) or by changing the height of the liquid level monitor as discussed in section 3.3.1.1. During the deposition of Cd-Fe-S films the spray rate was maintained constant at 2 cc/min.

#### 5.2.1.5 *Substrate temperature*

The Substrate temperature plays an important role in spray pyrolysis technique, as it affects the crystallinity and stoichiometry of the compound formation.

To optimise the substrate temperature, the spraying solution of fixed volumetric proportion and equal concentrations of individual ingredients was sprayed onto preheated glass substrates maintained at different temperatures. The substrate temperature was varied from 225 °C, at the interval of 25 °C, to 350 °C. During each deposition, the spray rate was maintained constant at 2 cc/min.

It was observed that the films deposited at temperatures 300 °C and 325 °C were uniform and adherent to the substrate. The electrical resistivity revealed that the films deposited at 325 °C show relatively lower resistivity. Hence 325 °C was considered to be the optimized temperature. The further deposition was taken at this optimized temperature by varying the volumetric proportions.

#### *5.2.1.6 Concentration of spraying solution*

The concentration of the solution also affects the properties of spray deposited thin films. The Cd-Fe-S thin films were prepared at constant optimized temperature for various concentrations of spraying solution. The concentrations were varied from 0.1 M, at the interval of 0.025 M to 0.025 M. The solution concentration was optimized to be 0.05 M as discussed in section 3.3.1.3.

### **5.2.2. CHARACTERIZATION OF Cd-Fe-S THIN FILMS**

The Cd-Fe-S thin films prepared at optimized preparative conditions were characterized by using X-ray diffraction, optical microscopy, dark resistivity and TEP techniques.

#### *5.2.2.1 X-ray diffraction*

XRD studies were carried out as discussed in section 3.3.2.2.

#### *5.2.2.2 Energy dispersive X-ray spectroscopy*

A compositional analysis of the deposited film material was carried out by energy dispersive X-ray analysis (EDAX) technique using KEVEX machine attached to SEM-PRO Model SU-30 by CAMECA.

#### *5.2.2.3 Optical microscopy*

Optical microscopy studies were carried out as discussed in section 3.2.2.3 to study surface morphology of Cd-Fe-S films.

#### *5.2.2.4 Optical absorption*

The same procedure to that discussed in section 3.2.2.4 was used to study the optical absorption of Cd-Fe-S thin films.

#### *5.2.2.5 Electrical resistivity*

Study of electrical resistivity was carried out in a similar manner to that discussed in section 3.2.2.5.

#### *5.2.2.5 Thermoelectric power (TEP)*

Thermoelectric power measurements were performed as discussed in section 3.2.2.6.

### **5.3 RESULTS AND DISCUSSION**

The thickness of the prepared film is determined by using relation (2.1), by a gravimetric weight difference method. The density of deposited material is considered to be the average density of bulk CdS and FeS materials ( $4.75 \text{ gm/cm}^3$ ). The thickness of a typical Cd-Fe-S film is found to be  $0.47 \mu\text{m}$ .

#### ***5.3.1 X - RAY DIFFRACTION (XRD)***

Fig. 5.1 shows XRD patterns of the Cd-Fe-S thin films for three different compositions of Cd:Fe. It is observed that the material is showing crystallinity for 8:2 proportion of Cd:Fe but for further increase of Fe proportion such as 6:4, 4:6, 2:8, and 10:0, the material remains amorphous. The XRD peaks as obtained for the 8:2 proportion match to that with ASTM data for CdS [12]. However, there is no peak corresponding to Fe. This may

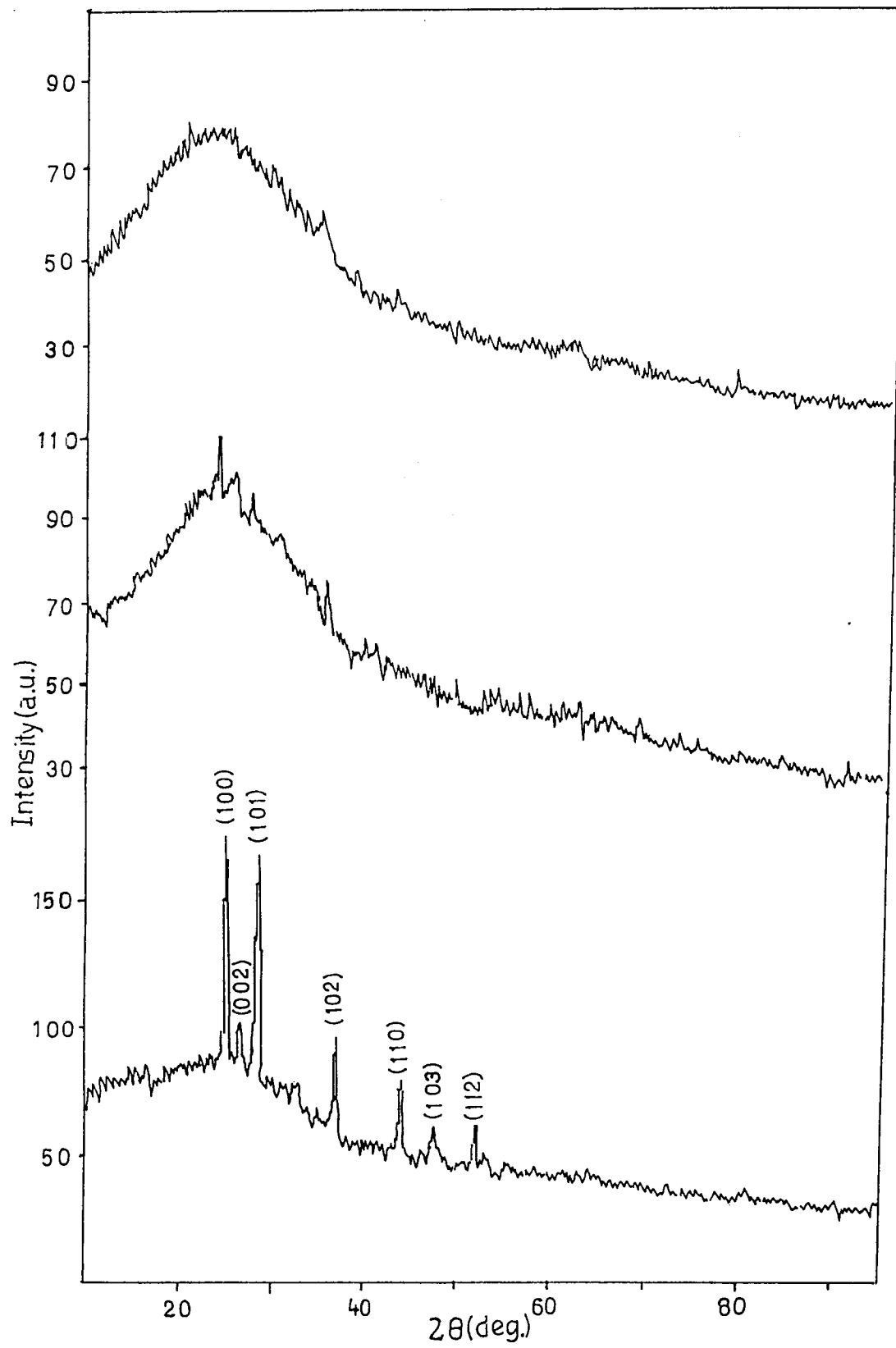


**Fig. 5.1** : XRD patterns of Cd-Fe-S for compositions a) 8:2, b) 6:4 and c) 4:6

be due to the fact that Fe is engaged in amorphous FeS phase. For ensuring the presence of proper proportion of Fe in Cd-Fe-S films, the film was characterized by EDAX technique discussed in next section. Table 1 shows matching of observed and standard 'd' values for the Cd-Fe-S films with 8:2 proportions of Cd and Fe.

**Table 1.** Comparison of observed and standard 'd' values for Cd - Fe - S thin film with 8:2 proportions

Observed 'd' values Å	Standard 'd' values Å	planes (hkl)
3.572	3.583	(100)
3.346	3.357	(0020)
3.154	3.160	(101)
2.432	2.450	(102)
2.063	2.068	(110)
1.912	1.898	(103)
1.750	1.761	(112)

### 5.3.2 ENERGY DISPERSIVE X-RAY SPECTROSCOPY

The compositional analysis of an optimized Cd - Fe - S film with 8:2 proportion of Cd:Fe is carried out by energy dispersive X-ray spectroscopy technique. From the EDAX data the atomic weight percentage of the elements is obtained as follows:



Cd - 43.6 % ( $\pm 1\%$ )

Fe - 14.6 % ( $\pm 1\%$ )

S - 41.6 % ( $\pm 1\%$ )

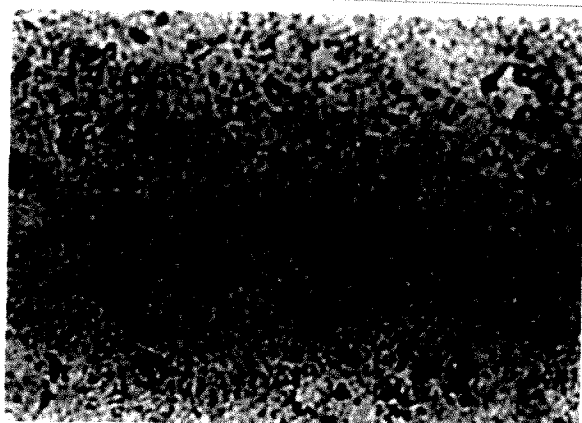
From the above values it is observed that the films contain acceptable proportion of Fe. However, the films are deficient in sulfur and the proportion of various elements deviates from the expected 8:2:10 proportion.

### ***5.3.3 OPTICAL MICROSCOPY***

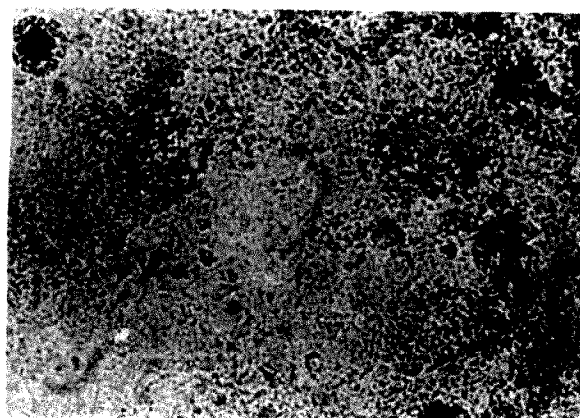
Fig. 5.2 shows optical micrographs of Cd-Fe-S thin films for three typical Cd:Fe proportions. From the micrographs, it can be seen that the films are continuous, covering entire substrate surface and are pinhole free. The micrographs clearly show that as the Fe proportion goes on increasing, the grains start on disappearing and the material shifts towards amorphous side. This has been evidenced by the XRD studies also.

### ***5.3.4 OPTICAL ABSORPTION***

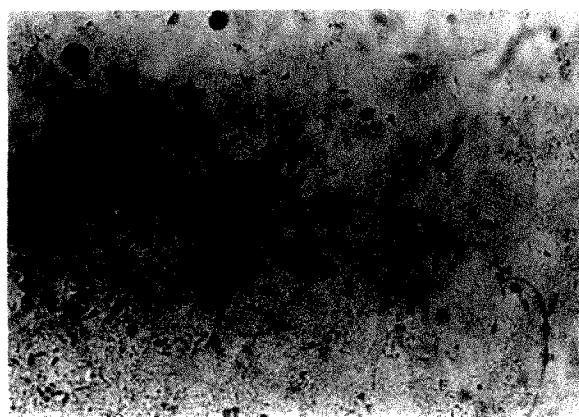
Fig. 5.3 shows the variation of optical density ( $\alpha t$ ) with wavelength ( $\lambda$ ) for the Cd-Fe-S thin films of various compositions. The absorption coefficient ' $\alpha$ ' is found to be of the order of  $10^4 \text{ cm}^{-1}$ . Following the theoretical analysis, the energy dependence of absorption coefficient can be expressed by the relation (2.8) for amorphous semiconductors [13-20] with  $n = 2$ .



a



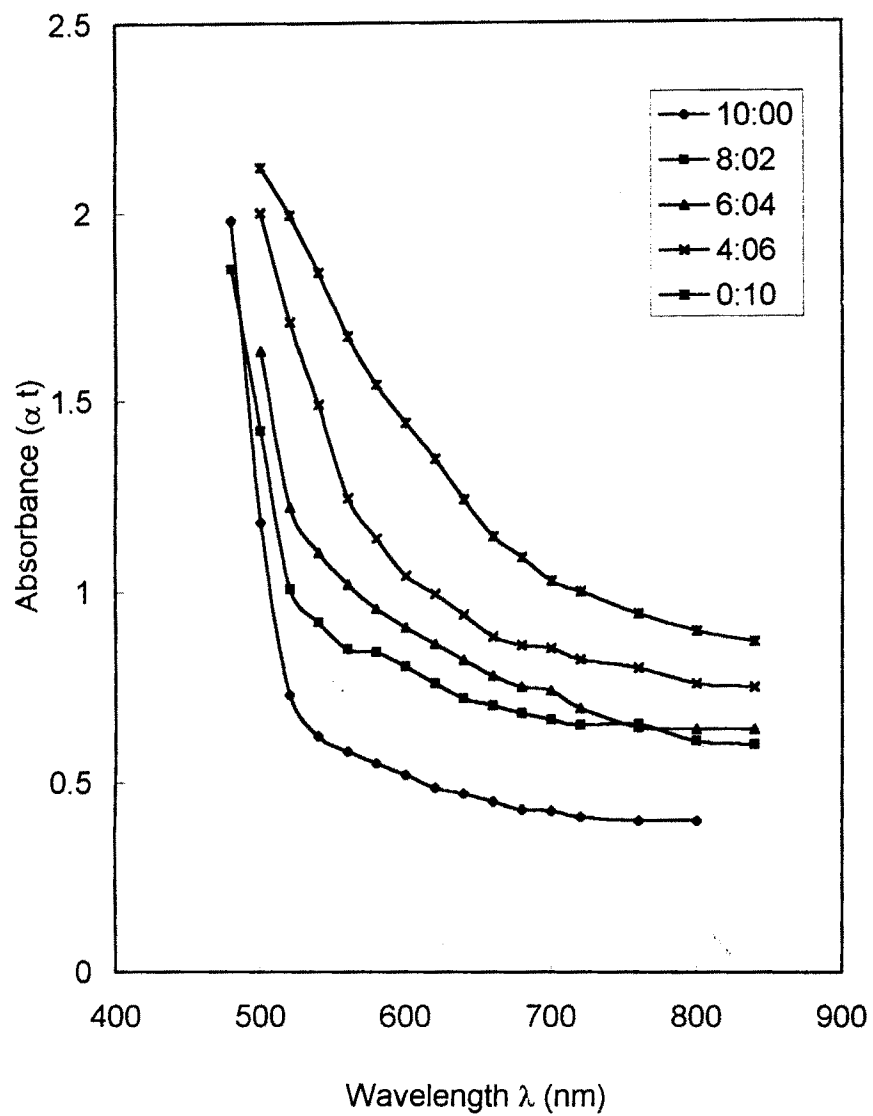
b



c

**Fig. 5.2:** Optical micrographs of Cd-Fe-S films for compositions :

a) 8:2, b) 6:4 and c) 4:6



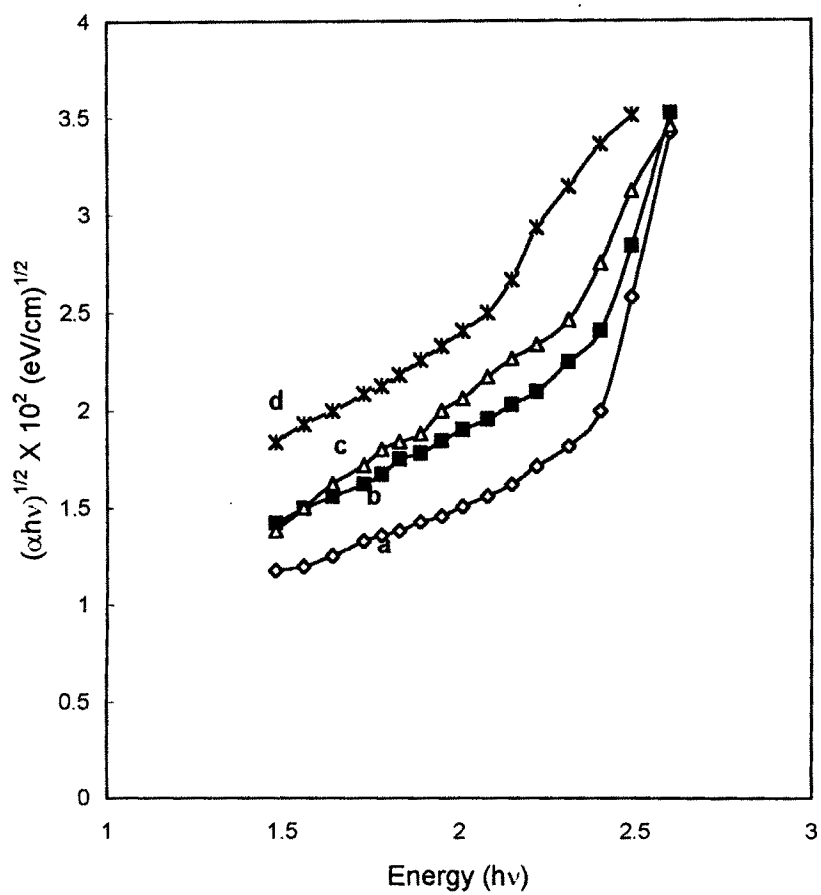
**Fig. 5.3** Plots of absorbance ( $\alpha t$ ) vs. wavelength ( $\lambda$ ) for different Cd:Fe proportions in Cd-Fe-S films

Fig. 5.4 shows the graph of  $(\alpha h\nu)^{1/2}$  versus  $(h\nu)$  for some typical Cd-Fe-S films with different proportions of Cd:Fe. The optical gap is determined by extrapolating straight-line portion of the graphs to  $\alpha = 0$ . It is observed that the optical gap decreases with increase in proportion of Fe in Cd-Fe-S. Thus the variation of Fe content in Cd-Fe-S has better control over the optical gap. Similar results have been reported earlier for  $\text{Cd}_x\text{Zn}_{1-x}\text{S}$  and  $(\text{CdS})_x(\text{Bi}_2\text{S}_3)_{1-x}$  [21,22]. The variation in optical gap is in between the individual band gaps of CdS and FeS. This is in agreement with the fact that the band gap of a ternary semiconductor lies in between the individual components forming a ternary semiconductor [23].

### 5.3.5 ELECTRICAL RESISTIVITY

The electrical resistivity measurements performed by using d.c two points probe method indicate that the Cd-Fe-S films are highly resistive. The room temperature resistivity of the films ranges from  $10^4 \Omega \text{ cm}$  to  $10^5 \Omega \text{ cm}$  as the composition varies from 8:2 to 2:8 of Cd: Fe.

The high resistivity at room temperature and increase in resistivity with increase in proportion of Fe in Cd-Fe-S films may be due to decrease in crystallinity of the films or change to the amorphous nature of the films with increase in Fe content.



**Fig. 5.4** Plots of  $(\alpha hv)^{1/2}$  versus  $hv$  for Cd-Fe-S films  
a) 10:0, b) 8:2, c) 6:4, d) 0:10

Fig 5.5 depicts the plots of  $\log \rho$  versus  $(1000 / T)$ . It is observed from the nature of the graphs that the resistivity of the films decreases with increase in temperature indicating that the material is semiconducting. The activation energy of the films is calculated from the resistivity plots and is found to be increasing with increase in Fe content in Cd-Fe-S films. The activation energies for different proportions of Cd and Fe are given in table 2.

**Table 2:** Activation energy and room temperature resistivity for Cd-Fe-S films.

Cd : Fe Proportion	Activation energy (eV)	Room temp resistivity $\Omega$ cm
8:2	0.37	$1.4 \times 10^4$
6:4	0.45	$1.4 \times 10^4$
2:8	0.49	$1.4 \times 10^5$

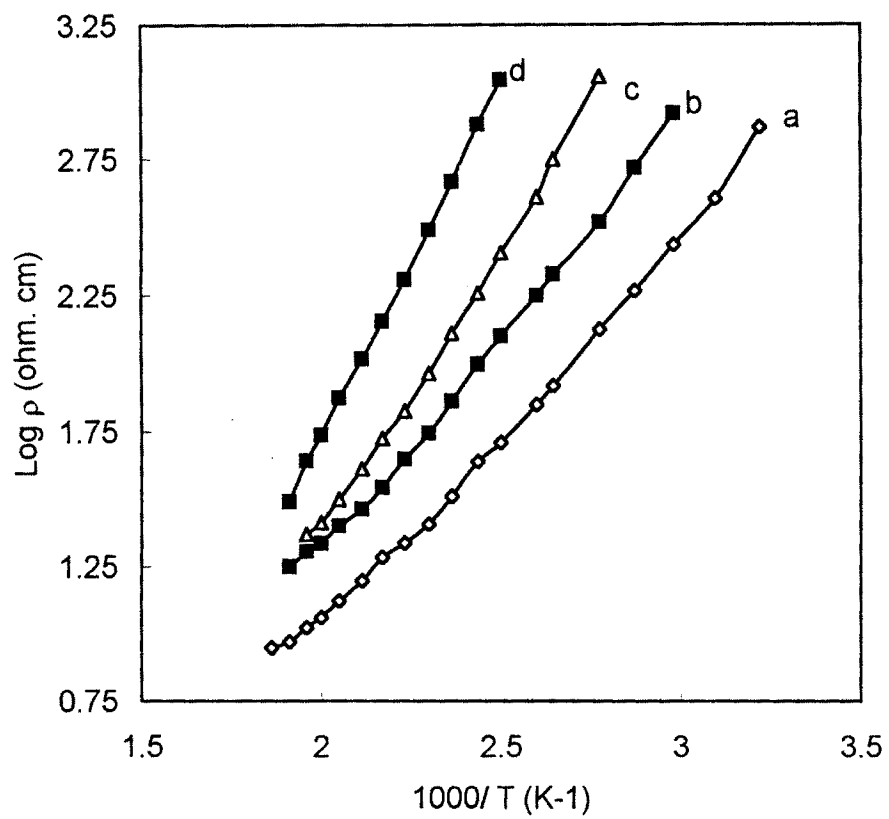


**Fig 5.5** Plots of  $\log \rho$  versus  $100/T$  for Cd-Fe-S thin films with different compositions of Cd:Fe a) 10:0, b) 8:2, c) 6:4, d) 0:10

### 5.3.6 THERMOELECTRIC POWER (TEP)

Thermoemf measurements for the Cd-Fe-S films are carried out in the temperature range of 300 K to 425 K. The dependence of thermoemf on temperature difference is depicted in Fig. 5.6 for Cd-Fe-S films with different proportions of Cd and Fe. It is observed that polarity of thermally generated voltage is positive towards the hot end indicating that the material is n-type. The plots show that increase in temperature difference leads to increase in thermoemf. This may be due to the fact that at higher temperature difference between the hot and cold ends, the temperature gradients is increased. This higher temperature gradient causes more charge carries to be diffused from hot to the cold end thereby establishing higher thermoemf between the hot and cold ends.

It is also observed that the thermoemf varies with Fe proportion in Cd-Fe-S films. As the proportion of Fe increases the thermoemf decreases; for a particular temperature difference. This may be due to following reason. As the proportion of Fe in Cd-Fe-S increases, more and more number of sulfur ions associate (bonding) with Fe ions to form FeS, which remains in amorphous phase. Thus the proportion of CdS in the film, which is crystalline, is decreasing with increased Fe proportion. As a consequence, the number of free charge carriers available for conduction is also decreasing. This leads to decrease in thermoemf with increase in Fe content in Cd-Fe-S.



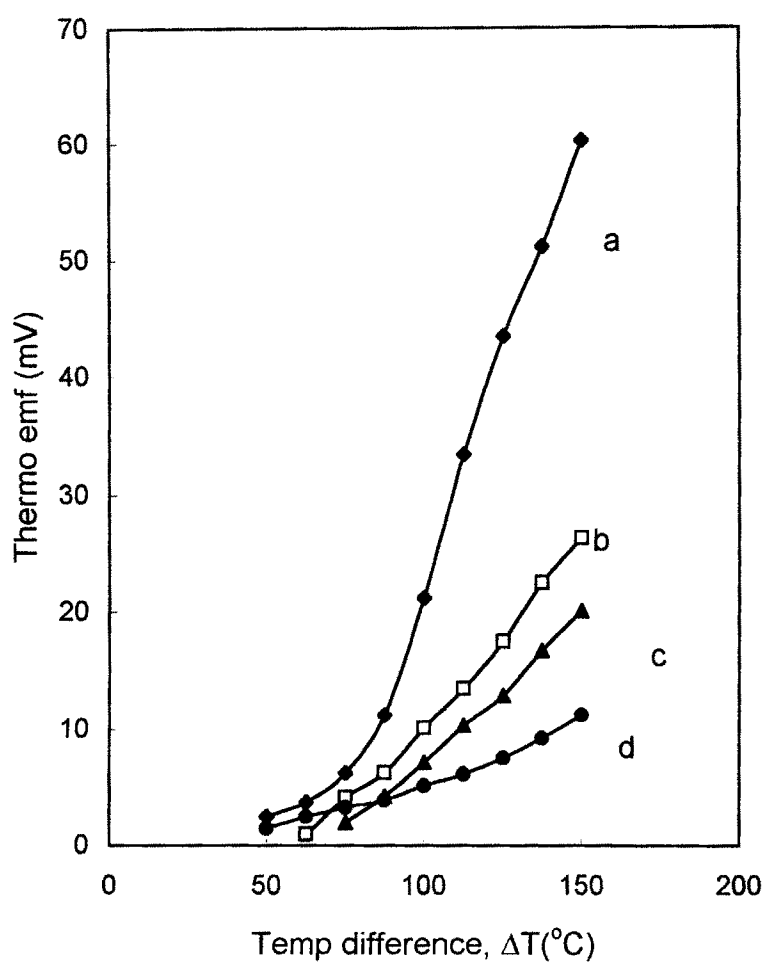


Fig. 5.6 Variation of thermoemf  $\Delta V$  with temperature difference  $\Delta T$  for Cd-Fe-S films with different proportions of Cd:Fe  
a) 10:0, b) 8:2, c) 6:4, d) 0:10

**REFERENCES**

1. N.R. Pawaskar, C.A. Menezes and A.P.B. Sinha, J. Electrochem. Soc., 124 (1997) 743.
2. K.L. Hardee and A.J. Brad, J. Electrochem. Soc., 122 (1975) 739.
3. H.M. Francombe, trans. 10<sup>th</sup> Natl. Vacuum symp. The Mc Millan Company, New York (1963)
4. C.H. Bhosale, M.D. Uplane, P.S. Patil and C.D. Lokhande, Thin Solid films, 248 (1994) 137
5. H.S. Soni, S.D. Sataye and A.P.B. Sinha, Ind. J. Pure. Appl. Phys., 21 (1982) 197
6. S.K. Pawar and S.H. Pawar, Mat. Res. Bull. 18 (1983) 211.
7. H. Tsuiski, H. Minoura, T. Nakomura and Y. Ueno, J. Appl. Electrochem., 8 (1978) 523
8. C.J. Liu. and J.H. Wang , phys. Lett., 36 (1980) 852.
9. S.H. Pawa , S.P. Tamhankar and C.D. Lokhande, J. Electrochem. Soc., 132 (1985) 262.
10. S.H. Pawar, C.H. Bhosale and A.J. Pawar, Ind. J. Pure Appl. Phys., 26 (1988) 323
11. S.H. Pawar, S.P. Tamhankar and C.D. Lokhande, Mater. Chem. Phys., 11 (1984) 401
12. ASTM data file card No. 6 - 0314

13. C. Wood, L.R. Gilbert, V. Von pelt and woolffing, *Phys. Status Solidi (b)*, 68 (1975) K 39
14. T. Fujita, K. Kurita, K. Takiyama and T. Oda, *J. Phys. Soc. Japan*, 56 (1987) 3737
15. T. Fujita, K. Kurita, K. Takiyama and T. Oda, *J. Lumin*, 39 (1998) 175.
16. H.S. Soliman, W.Z. Soliman, M.M. El- Nahas and Kh. A. Mady, *Optica Pura Y. Applicada*, 22 (1989) 115
17. K. Shimakawa, *J. Non-Cryst. Solids*, 10 (1988) 151
18. K. Shimkawa, *J. Non-Cryst. Solids* 43 (1981) 229
19. L. Tichy and A. Triska, *Solid State Commun.*, 41 (1982) 751
20. C. Wood, L.R. Gilbert, R. Mueller and C.M. Garner, *J. Vac. Sci. Technol.*, 10 (1973) 739
21. G.K. Padam, G.L Malhotra, S.U.M. Rao, *J. Appl. Phys.*, 63 (1988) 770
22. Wolf H.F., *Semiconductors*, Wiley Interscience, USA (1971)
23. R.R. Ahire, M.Phil Thesis, Shivaji University, Kolhapur (India) (2001)